Gasdynamic characteristics of toroidal shock and detonation wave converging

TENG Honghui[1,2] & JIANG Zonglin[2]

1. Key Laboratory of High Temperature Gas Dynamics, Institute of Mechanics, Chinese Academy of Sciences, Beijing 100080, China;
2. Graduate University of Chinese Academy of Sciences, Beijing 100039, China
Correspondence should be addressed to Teng Honghui (email: hhteng@ustc.edu; honghuiteng@ gmail.com)

Abstract The modified CCW relation is applied to analyzing the shock, detonation wave converging and the role of chemical reactions in the process. Results indicate that the shock wave is strengthened faster than the detonation wave in the converging at the same initial Mach number. Euler equations implemented with a detailed chemical reaction model are solved to simulate toroidal shock and detonation wave converging. Gasdynamic characteristics of the converging are investigated, including wave interaction patterns, observable discrepancies and physical phenomena behind them. By comparing wave diffractions, converging processes and pressure evolutions in the focusing area, the different effects of chemical reactions on diffracting and converging processes are discussed and the analytic conclusion is demonstrated through the observation of numerical simulations.

Shock wave focusing is a fundamental problem in the shock wave research and the instantaneous impulse of high temperature and pressure generated at the focal points has been applied recently in industrial and medical researches[1]. There are several methods to create shock wave focusing, among which the more commonly-used one is to make a planar shock wave reflect from a concave surface, such as the elliptical or parabolic reflector. Toroidal shock wave focusing has been proposed and investigated in recent years, for which there is no need for a reflector and no change in the shock propagation direction. Moreover, the focusing is three dimensional, and therefore, much stronger focusing can be expected. Jiang and Takayama[2] numerically simulated the toroidal shock wave diffracting and focusing in an unconfined space, and reported that the incident shock converging at higher Mach number will induce more complicated shock reflection pattern. Hosseini et al.[3] experimentally investigated the focusing of a toroidal shock wave at a Mach number of 1.5 using a vertical co-axial diaphragmless shock tube,

and presented holographic interferograms at different moments as well as pressure histories measured on tube walls. Because of the area-converging in shock propagation direction, the incident shock will get stronger and stronger, and the post-shock pressure and temperature will arise higher and higher. For a given focusing method, the incident shock Mach number is a critical factor that affects the final post-shock flow state at focal points. Generally speaking, the stronger incident shock wave is necessary to create the higher focal pressure and temperature. However, in engineering application as well as scientific experiments, it is not so easy to obtain high Mach number shock wave with good reproductive ability. The situation embarrasses the applications of shock wave focusing. In this paper, detonation waves are recommended to facilitate the focusing of strong shock waves because even at the atmospheric pressure detonating a combustible gas mixture can generate strong shock waves, e.g. the detonation generated in stoichiometric hydrogen-air mixtures at one atm has a C-J Mach number about 5.1. To gain better understanding on detonation focusing, the shock and detonation wave converging are analyzed based on shock wave theories, and then the toroidal shock and detonation wave focusing are numerically simulated. From numerical results, wave interaction patterns, the post-shock pressure, and gasdynamic properties are investigated by comparing one case with the other. Discrepancies observed in each case and physical phenomena behind them are discussed.

1   Dynamic analysis of shock and detonation converging

The sketches of toroidal shock and detonation wave focusing and the computational domain are shown in Fig. 1. The tube complex consists of a circular shock tube and a solid cylinder, whose diameter rate is D: d = 0.2 m: 0.18 m. The incident shock or detonation wave propagates in the co-axial tube at first, as shown in Fig. 1(a), diffracts at the end of the solid cylinder, then converges toward the axis of symmetry, and finally focuses at their focal points. The toroidal wave focusing occurs on a line rather than a plane in planar cases, so it would be more effective to elevate the post-shock flow state near focal points. Furthermore, there are no reflectors in the converging process, and the main shock propagation direction remains unchanged. On the other hand, due to different physical essences of shock and detonation waves, there must be some different gasdynamic features being observable in their converging. Assuming that both shock and detonation waves propagate at the same Mach number in the co-axial tube, the converging process, wave reflection patterns and the focusing pressure around focal points are investigated in detail, and the qualitative conclusions related with their own features are reached.

The CCW relation[4], deduced by Chester (1954), Chisnell (1957), and Whitham (1958) independently, is one of the important equations in shock theories and describes Mach number variation with the wave surface area normal to shock propagation direction in a homogeneous static gas. Taking account of chemical reactions and the heat release, Li et al.[5] deduced the modified CCW relation which is applicable to detonation wave converging. The relation reads
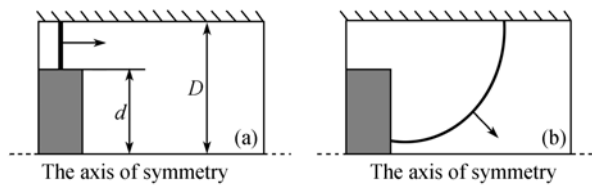
Fig. 1.   The sketches of toroidal shock or detonation wave focusing and their computation domains.

$$\frac{2MdM}{(M^2-\lambda)K(M)}+\frac{dA}{A}=0,\tag{1}$$

where

$$K(M)=2\sigma\left\{1+\mu(1+\sigma)+\frac{\lambda}{M^2}\left[1+\mu(1-\sigma)\right]\right\}^{-1}\left[1+\frac{(1+\sigma)\left(1-\mu^2\right)}{\sigma(1+\gamma_1)\mu}\right]^{-1},\tag{2}$$

$$\sigma=\left[1-\frac{2\left(\gamma_1^2-1\right)(q+\eta)M^2}{\left(M^2-\lambda\right)^2}\right]^{1/2},\tag{3}$$

$$\mu=\left[\frac{(\gamma_1-\sigma)M^2+\lambda(1+\sigma)}{(1+\sigma)\gamma_1 M^2-\lambda(\gamma\sigma+1)}\right]^{1/2},\tag{4}$$

$$\lambda=\frac{\gamma_1}{\gamma_0},\tag{5}$$

$$q=\frac{\gamma_1^2\left(\gamma_0-1\right)+2\gamma_0\left(\gamma_0-\gamma_1^2\right)M_{CJ}^2+\gamma_0^2\left(\gamma_0-1\right)M_{CJ}^4}{2\gamma_0^2\left(\gamma_0-1\right)\left(\gamma_1^2-1\right)M_{CJ}^2},\tag{6}$$

$$\eta=\frac{\gamma_1-\gamma_0}{\gamma_0\left(\gamma_0-1\right)\left(\gamma_1-1\right)},\tag{7}$$

where γ_0 and γ_1 are specific heat ratios in front of and behind a wave front, respectively. M_{CJ} denotes the Mach number of a CJ detonation wave, q is the chemical heat released in chemical reactions. For shock waves $K(M)$ is a slowly varying function of the Mach number, and for detonation waves it is also a function of the specific heat ratios and the chemical heat release. If $\gamma_0=\gamma_1$, $q=0$, the relation will be reduced to the classic CCW relation for shock waves. Li et al.[6] developed their two- and three-shock theories based on this modified CCW relation, and the oblique detonation reflection was investigated based on the theories. Their results show that the reflection is very sensitive to the intensity of overdriven detonations. The comparison between their analytical results and different numerical results or experimental data from other research groups indicates good

agreement.

In a standard stoichiometric hydrogen-air mixture, the function $K(M)$ of a shock wave ($\gamma_0 = \gamma_1 = 1.40$) or a detonation wave ($\gamma_0 = 1.40$, $\gamma_1 = 1.17$, $M_{CJ} = 5.1$) is shown in Fig. 2(a). The figure shows that the shock curve goes lower as the Mach number increases, and the detonation curve with the initial zero value at the CJ point goes up as the Mach number increases. Under given conditions the detonation curve is always lower than the shock curve. The Mach number variation with the wave surface area can be calculated by integrating eq. (1) from the CJ point, and the obtained result is plotted in Fig. 2(b). With the same initial Mach number and wave surface area, the figure shows that the Mach number in the shock case is much higher than the detonation one, and increases faster. Thus, it can be concluded that the post-shock pressure and temperature generated from shock focusing are higher than that from detonation focusing. This conclusion is drawn from the case of the hydrogen-air mixture, in which the function value $K(M)$ of the detonation is always smaller than that of the shock wave due to bigger molecules generated in reactions. In the case of hydrocarbon fuel gas mixtures with a low specific heat ratio, it is possible that the specific heat ratio of the product gas mixture is bigger than that of the reactant if the fuel mass fraction is large enough. Then, as Mach number increases the function value of $K(M)$ for detonations may finally become bigger than the shock wave case, which will result in an intersection between two $K(M)$ curves. For example, for the propane-oxygen mixture with an equivalence ratio of 3∶1 and specific heat ratios of $\gamma_0 = 1.217$ and $\gamma_1 = 1.28$, the intersection appears at the Mach number of 15.7. After the intersection point, the detonation Mach number increases faster than the shock wave during converging process. At the moment, the corresponding wave surface ratio is 0.025 for the shock wave case and 0.007 for the detonation. These two values are quite small, therefore, even for the gas mixture whose product specific heat ratio is higher
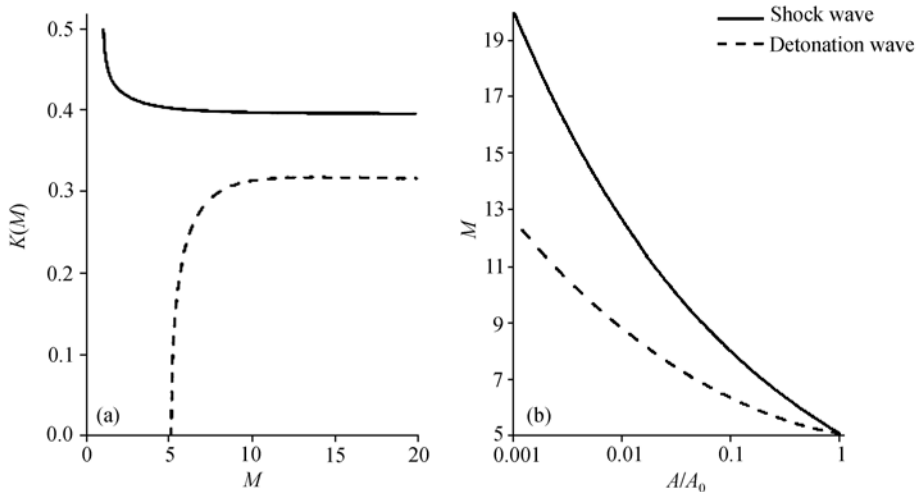

Fig. 2.   Dynamic characteristics of shock and detonation wave converging: (a) $K(M)$ as function of M; (b) Relation between M and wave surface area.

than the reactant, the Mach number increases faster for shock waves than detonations during the most portion of the converging process from their initial stage.

In the modified CCW relation the specific heat rate of the gas mixtures in reaction plays an important role in detonation converging. The lower specific heat ratio of a detonation product will result in less intensive focusing; while the higher one benefits the focusing. However, even as to the higher specific heat ratio the shock wave focusing appears much stronger than detonation waves during the most portion of the converging process from the initial stage. It should be noted that the modified CCW relation is derived based on the CJ theory, whereas the heat-releasing rate and gas dissociation related with the varying Mach number and expansion waves following detonation fronts are not considered. These factors limit the CCW relation's application near focal points. In the following sections, direct numerical simulations are carried out to gain deeper insight into the wave converging.

2 Numerical simulation of toroidal shock/detonation wave focusing

2.1 Governing equations and numerical methods

Assuming that dissipative effects, including viscosity, heat-conduction and diffusion, are neglected, the gaseous detonations are governed by two-dimensional multi-component Euler equations with chemical reaction terms. The equations can be written in conservation form with n continuity equations for a perfect gaseous mixture in Cartesian coordinates

$$\frac{\partial U}{\partial t} + \frac{\partial F}{\partial x} + \frac{\partial G}{\partial r} + \frac{k}{r} S = S_c, \tag{8}$$

where

$$U = \begin{bmatrix} \rho_1 & \rho_2 & \cdots & \rho_n & \rho u & \rho v & e \end{bmatrix}^T, \tag{9}$$

$$F = \begin{bmatrix} \rho_1 u & \rho_2 u & \cdots & \rho_n u & \rho u^2 + p & \rho uv & (e+p)u \end{bmatrix}^T, \tag{10}$$

$$G = \begin{bmatrix} \rho_1 v & \rho_2 v & \cdots & \rho_n v & \rho uv & \rho v^2 + p & (e+p)v \end{bmatrix}^T, \tag{11}$$

$$S = \begin{bmatrix} \rho_1 v & \rho_2 v & \cdots & \rho_n v & \rho uv & \rho v^2 & (e+p)v \end{bmatrix}^T, \tag{12}$$

$$S_c = \begin{bmatrix} \dot{\omega}_1 & \dot{\omega}_2 & \cdots & \dot{\omega}_n & 0 & 0 & 0 \end{bmatrix}^T. \tag{13}$$

In eq. (8), $k = 1$ is for axisymmetric flows and $k = 0$ for planar ones. $\rho_i (i=1, \ldots, n)$ is the i-th specie density, the total density $\rho = \sum_{i=1}^{n} \rho_i$, u and v are velocities in x- and

r-direction, respectively. *e* denotes total specific energy defined by $e = \rho h - p + 1/2$ $\times \rho(u^2 + v^2)$, where $h = \sum_{i=1}^{n} \rho_i h_i / \rho$ and h_i is calculated with curve fitting. $p = \sum_{i=1}^{n} \rho_i R_i T$ and R_i is the *i*-th specie gas constant. $\dot{\omega}_i$ is the mass production rate of the *i*-th specie.

Dispersion Controlled Dissipation (DCD)[7] Scheme is used to discretize the governing equations. It is one kind of the TVD schemes and constructed based on the dispersion control conditions. To account for chemical reactions in detonations, 9 species (H_2, O_2, O, H, OH, HO_2, H_2O_2, H_2O, Ar) and 19 reactions are considered in a chemical reaction model. The time splitting method is used to overcome the stiff problem arising from chemical reaction calculations. The inflow and outflow boundaries are specified with the nonreflecting condition, and the reflection condition is applied at both walls and the axis of symmetry. The initial conditions for both shock waves and detonations are 32 kPa, 298.15 K, $2H_2+O_2+7Ar$. In detonation simulation, a steady CJ detonation wave obtained from one-dimensional calculation is initiated in the toroidal shock tube. In shock simulation, the incident shock wave is posited in the toroidal shock tube with a Mach number being the same as the CJ detonation, which is 4.8 for the prescribed gas. The simulation is carried out with the same numerical code for the detonation simulation, but $\dot{\omega}_i = 0$.

2.2   Wave interaction patterns in wave converging

Wave interaction patterns, shortly after diffracting and focusing processes start, are shown in Fig. 3. There are several discrepancies observable between the shock wave case, as shown in Figs. 3(a) and (b), and the detonation case, as shown in Figs. 3(c) and (d). First, pseudosteady expansion waves appear in front of the toroidal tube outlet in the shock wave case, but unsteady upstream expansion waves appear inside the toroidal tube in the detonation case, as shown in Figs. 3(a) and (c). Actually, for shock waves at a higher Mach number, e.g. higher than 2.068 at $\gamma = 1.40$, the supersonic flow will develop behind a shock front, therefore, disturbance cannot propagate upstream. For detonations, the gas temperature behind detonation fronts is very high and the flow is subsonic. No supersonic flow is generated even if there is a strong expansion during diffraction, therefore, any disturbance can travel upstream. Secondly, there is a secondary shock wave in the shock wave case, but not in the detonation one. The secondary shock wave develops due to the locally generated supersonic flow behind the diffracting wave. Analytical and experimental results[8] showed that if the incident shock Mach number is larger than 1.346 ($\gamma = 1.40$), there will be the secondary shock wave while shock waves diffract over a backward step. In the detonation case, the flow is subsonic behind the CJ
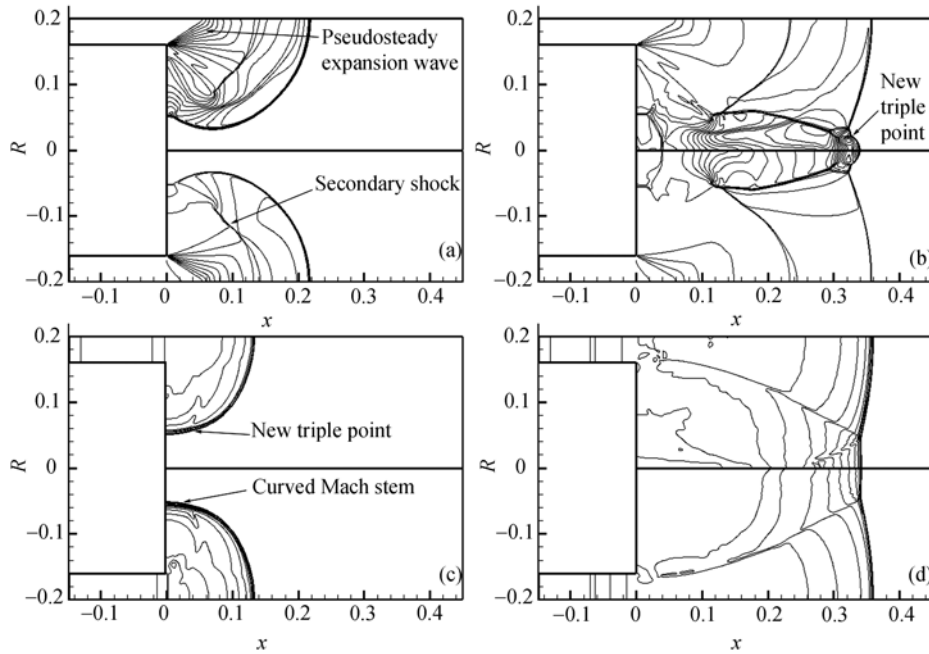
Fig. 3.   Density (upper) and pressure (lower) contours at two time instants with an initial incident Mach number of 4.8. (a) and (b) Shock; (c) and (d) detonation.

plane and the flow velocity decreases rapidly due to Taylor expansion waves, so there is no locally generated supersonic flow and then no secondary shock wave developed. Another discrepancy observable from the wave interaction patterns is the Mach reflection style at the end of the solid cylinder, as shown again in Figs. 3(a) and (c). A short Mach stem forms and lags behind the diffracting wave in the shock wave case. For the detonation case, a long Mach stem forms and bends forward. Detailed simulations show that the detonation decoupling and re-initiation occur here during detonation diffraction. Thus, the overdriven detonation induced by the detonation re-initiation results in the longer Mach stem and the stronger Mach reflection, as shown in Fig. 3(c).

After focusing on the axis of symmetry the Mach reflection patterns appear again, as shown in Fig. 3(b) for shock waves and in Fig. 3(d) for detonations. The shock wave Mach stem is curved forward and the detonation Mach stem is straight. Actually, at the beginning of the shock wave Mach reflection development, its stem is also straight, but bends forward and the part of it near the axis of symmetry gets semi-spherical. Near the intersection point of the semi-spherical Mach stem and the original one, there is a new triple point from which a shear layer develops. This Mach reflection pattern was referred to as the spherical double Mach reflection[9]. This wave interaction pattern is induced by a strong jet generated from focusing. The jet impacts on the Mach stem in front of it and reforms the Mach stem. The shock wave in the present study moves as if it is driven by a piston and the post-shock flow is homogeneous. As to the detonation it is self-sustained, and behind it there are Taylor expansion waves that adjust the post-detonation flow to

satisfy the zero boundary condition. Therefore, the jet in the detonation case is weaker due to Taylor expansion waves and there is no spherical double Mach reflection being observable.

2.3   Pressure variations during wave converging

Nondimensional pressure profiles along the axis of symmetry at several time instants shortly after focusing are shown in Fig. 4. Because the Mach stem near the wall lags behind the diffracting shock, as shown in Fig. 3(a), the diffracting shock wave focuses first on the axis of symmetry at a position about 0.08 from the end of the solid cylinder, in which a pressure peak is generated and moves forward, as shown in Fig. 4(a). As to the detonation case as shown in Fig. 4(b), the pressure peak is generated due to the collision of the Mach stem just at the end of the solid cylinder. The second pressure peak appears later near the end of the solid cylinder in the shock wave case, as shown in Fig. 4(a), and is generated by the Mach stem focusing. Both the positions were called the effective focal points in the toroidal shock wave focusing[10]. In the present simulation, the pressure value can reach 290.4 from the first focusing and 208.6 from the second one, as shown in Fig. 4(a). To investigate further into the two focal points, several cases with different initial toroidal shock Mach numbers were simulated. It is demonstrated that if the Mach number falls the first focal point will move backward and finally joint the second one, while if the Mach number arises the first focal point will move forward and the two focal points will become apart away further. The peak pressure due to each focusing will vary also with the Mach number, but the peak pressure from the second focusing can change more dramatically, for example, if the Mach number is above 5.0, the maximum pressure from the second focusing can be higher than that from the first one. Different from the shock wave focusing, there is only one focal point near the wall in the detonation wave focusing. As shown in Fig. 4(b), the high pressure induced by detonation focusing appears between 0 and 0.02, and the maximum peak value reaches 447.8, but it falls to 120 in about 5 microsecond. Further simulations show that the transition
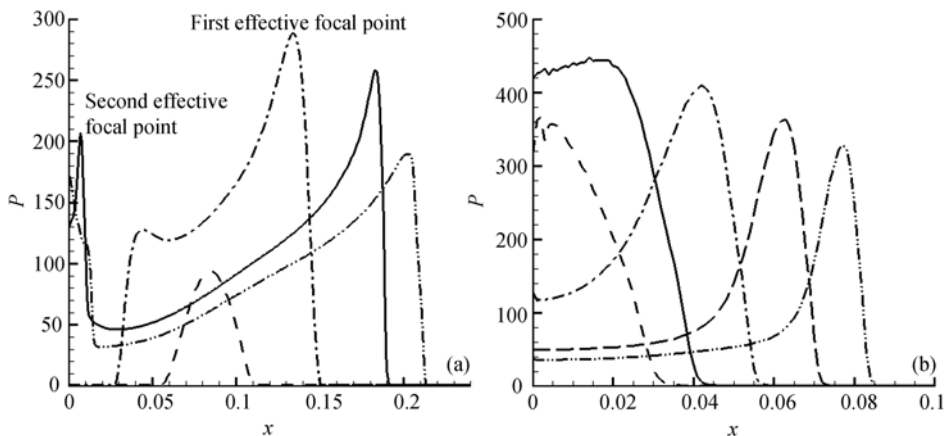

Fig. 4.   Nondimensional pressure profiles along the axis of symmetry at several time instants shortly after focusing: (a) shock; (b) detonation.

from the regular to Mach reflection takes place near 0.13. Since then, the detonation develops into CJ detonation gradually. The peak pressure falls relaxedly to 212.5 before the transition, and then drops more quickly after the transition. The pressure value falls to 37.9 when the wave front arrives at 0.25 and to 26.6 when the wave arrives at 0.4.

The toroidal shock/detonation wave motion in the present study experiences two wave processes: diffracting and converging. The two processes affect the flow state near the focal point in different ways, so it may be useful to examine their roles in focusing. The nondimensional pressure at the wave front, shortly after the diffraction process starts, is shown in Fig. 5 as a function of the diffraction angle. The diffraction angle is defined as the angle between the main flow direction and the line connecting the wave surface point and the backward step vertex. In the shock wave diffraction the pressure decreases as the diffraction angle increases because the flow expands more in the direction of a larger diffraction angle. Derived from the same mechanism the detonation pressure behaves in the same manner, but the corresponding pressure drop is much smaller than the shock wave. This is due to the contribution from the heat released from chemical reactions. Therefore, the pressure in the same diffraction angle is higher in the detonation front than in the shock front. Furthermore, the diffracting wave with a diffraction angle of 90º will focus on the axis of symmetry, in which direction the pressure has the most discrepancies. Therefore it can be concluded that the diffraction will result in weaker focusing for both the cases, but the diffracting detonation can induce more intensive focusing than the diffracting shock wave in the present study.
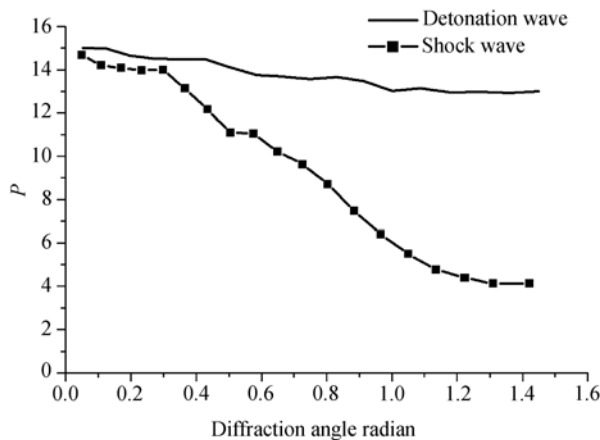

Fig. 5.   Nondimensional pressure at the wave front as a function of the diffraction angle shortly after the diffraction.

To examine the converging process a series of the pressure profiles at the end of the solid cylinder along the radical direction during converging of the diffracting shock/detonation are presented in Fig. 6. The figure shows that the pressure after the diffraction is much lower in the shock wave case than that in the detonation one. The pressure in the latter case is further elevated by the overdriven detonation induced by the detonation re-initiation during diffraction. Although the initial pressure value is lower in
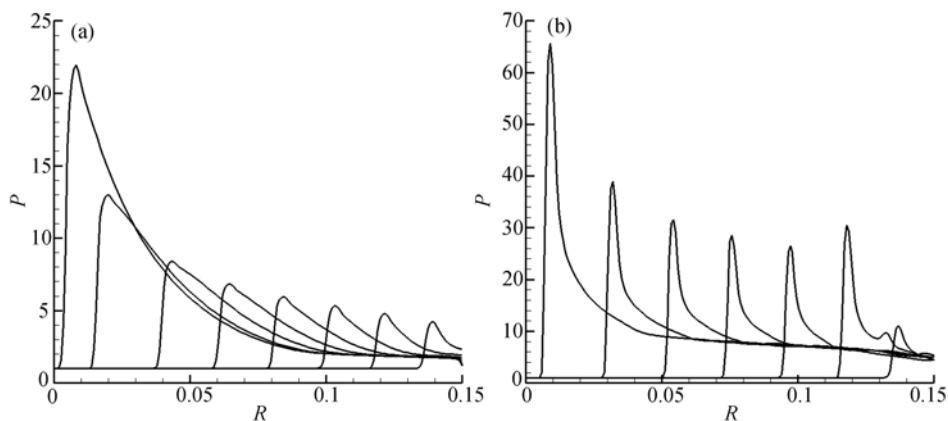
Fig. 6.   Nondimensional pressure at the end of the solid cylinder along the radical direction during converging: (a) shock; (b) detonation.

the shock wave case, the pressure increases more rapidly than that in the detonation case. To examine the pressure-increasing rate, the period when the wave front propagates from 0.1 to 0.0085 is chosen to study pressure variations. During this period the post-detonation pressure increases from 25.9 to 65.5 by about 2.5 times, while the post-shock pressure arises from 5.5 to 20.9 by about 3.8 times. Therefore, the post-shock pressure-increasing rate is 1.5 times higher than the post-detonation pressure. This demonstrates the conclusion drawn from the theoretical analysis. However, the pressure drop in the detonation diffraction is smaller and the diffracting detonation has a much higher initial pressure at the beginning of converging, so the final peak pressure near the focal point is much higher than the shock wave case. In conclusion, the detonation can result in the higher focal pressure than the shock wave for the same incident Mach number in the toroidal wave focusing, which indicates the potential application background.

3   Concluding remarks

Gasdynamic characteristics of the shock and detonation converging are analyzed by using the CCW relation, and the numerical simulations of toroidal shock and detonation waves converging are carried out by solving Euler equations implemented with a detailed chemical reaction model. The research work is summarized as follows:

1. Theoretical analysis shows that the shock wave converging can result in more intensive focusing than the detonation converging at the initial Mach number because the gas mixture specific heat ratio is changed during chemical reactions, and the conclusion is verified by numerical simulation results.

2. In the toroidal shock/detonation wave converging at the same initial Mach number, the detonation results in a higher pressure near the focal point than shock waves due to the less pressure drop during detonation diffraction.

3. With the same high Mach number, the post-shock flow is supersonic and homogeneous and the post-detonation flow is subsonic and nonhomogeneous, which results in

different wave interaction patterns in the two cases.

References

1. Takayama, K., Saito, T., Shock wave/geophysical and medicine applications, Annu. Rev. Fluid Mech., 2004, 36: 347   79.[DOI]
2. Jiang, Z., Takayama, K., Reflection and focusing of toroidal shock waves from coaxial annular shock tubes, Computers & Fluids, 1998, 27: 553   562.[DOI]
3. Hosseini, S., Takayama, K., Study of shock wave focusing and reflection over symmetrical axis of a compact vertical co-axial diaphragmless shock tube, Proceedings of ISSW23, 2001, 2: 1550   1557.
4. Han, Z. Y., Yin, X. Z., Shock Dynamics, Dordrecht: Kluwer Academic Publishers and Science Press, 1993: 21   41.
5. Li, H., Ben-Dor, G., A modified CCW theory for detonation waves, Combustion and Flame, 1998, 113: 1   12. [DOI]
6. Li, H., Ben-Dor, G., Grönig, H., Analytical study of the oblique reflection of detonation waves, AIAA Journal, 1997, 35(11): 1712   1720.
7. Jiang, Z., On dispersion-controlled principles for non-oscillatory shock-capturing schemes, Acta Mechanica Sinica, 2004, 20(1): 1   15.
8. Sun, M., Takayama, K., The formation of a secondary shock wave behind a shock wave diffracting at a convex corner, Shock Waves, 1997, 7: 287   295.[DOI]
9. Jiang, Z., Takayama, K., Reflection and focusing of toroidal shock waves from coaxial annular shock tubes, Computers & Fluids, 1998, 27: 553   562.[DOI]
10. Teng, H., Jiang, Z., Han, Z. Y., Numerical investigation of diffraction, focusing and reflection of toroidal shock waves, Acta Mechanics Sinica (in Chinese), 2004, 36(1): 9   15.